PROCEEDINGS OF SCIENCE

Top quark physics in the ATLAS detector: summary of Run I results

María Moreno Llácer[*†]
II. Physikalisches Institut, Georg-August-Universität Göttingen, Friedrich-Hund-Platz 1, D-37077 Göttingen, Germany
E-mail: maria.moreno.llacer@cern.ch

An overview of the most recent results on top quark physics obtained using proton-proton collision data collected with the ATLAS detector at the Large Hadron Collider at $\sqrt{s}$ = 7 TeV or $\sqrt{s}$ = 8 TeV centre-of-mass energy are presented. Measurements for inclusive and differential top quark pair and single top quark production in different final states are reviewed. The latest measurements of the top quark mass, top quark properties such as charge asymmetry and spin correlations, constraints on the coupling of the top quark to the W boson and the recent evidence of top quark pairs produced in associated with vector bosons are also presented.

ATL-PHYS-PROC-2015-011
28 March 2015

Proceedings of the Corfu Summer Institute 2014 "School and Workshops on Elementary Particle Physics and Gravity",
3-21 September 2014
Corfu, Greece

[*]Speaker.
[†]on behalf of the ATLAS Collaboration

PoS(CORFU2014)082

1. Introduction

The Large Hadron Collider (LHC) has performed extraordinarily well throughout 2011 and 2012 providing both the ATLAS [1] and the CMS [2] experiments with over ten million top quarks each. The top quark is one of its kind - it is the heaviest elementary particle ever observed, with a mass of the order of an entire atom of gold-. With a charge of +2/3$|e|$ (e is the electron charge) and spin 1/2, it completes the third family structure of the Standard Model (SM). Top quarks show remarkable distinctive features when compared to the other quarks. Due to its large mass, it has such a large decay width ($l = \frac{\gamma\beta c\hbar}{\Gamma_t} \approx 0.2$ fm) that it decays before traversing any significant distance to disturb the colour field giving rise to non-perturbative effects such as its fragmentation and hadronization. Therefore all properties of the "naked" quark are preserved in the decay chain of a top quark and propagated to its decay products. In the SM, top quarks are expected to decay mostly through $t \to Wb$, being the branching ratios Br($t \to Ws$) $\sim 0.18\%$ and Br($t \to Wd$) $\sim 0.02\%$ negligible compared to the dominant decay channel [3]. Furthermore, its mass is close to the electroweak symmetry breaking mechanism scale, so it is likely that the top quark plays a special role in this mechanism. The Tevatron and LHC experiments have eagerly analysed the data they have collected seeking to understand better the top quark production and its basic properties. In these proceedings a selection of such rich top quark programme is presented highlighting the most recent results obtained by the ATLAS collaboration.

2. Top quark production

Within the SM, top quarks are produced either in pairs via the strong interaction ($t\bar{t}$ production) or as single top quarks via the electroweak interaction. Each top quark decays almost 100% of the time to a W boson and a b quark. The W bosons can decay leptonically into an electron, muon or tau and the corresponding neutrino, or hadronically into quark-antiquark pairs. Thus, the final states of $t\bar{t}$ events are subdivided into the dilepton channels with both W bosons decaying leptonically, the lepton+jets channels in which one of the W bosons decays leptonically and the other one hadronically, and the all hadronic channel with both W bosons decay hadronically.

2.1 Top quark pairs (strong interaction)

In hadron colliders, the top quarks are predominantly produced in pairs via the strong interaction, through gluon-gluon fusion or quark-antiquark annihilation. At the LHC (unlike the Tevatron) the former mechanism dominates, contributing by a factor $\sim$80% to the total top quark pair production cross section.

The calculation of the top quark pair cross section has recently been completed, after long standing theoretical efforts, to exact next-to-next-to leading order (NNLO) in QCD including resummation of next-to-next-to-leading logarithmic (NNLL) soft gluon terms. The NNLO+NNLL $t\bar{t}$ cross section for pp collisions is $\sigma_{t\bar{t}} = 177^{+10}_{-11}$ pb at $\sqrt{s}$ =7 TeV and $\sigma_{t\bar{t}} = 253^{+13}_{-15}$ pb at $\sqrt{s}$ =8 TeV for a top quark mass of 172.5 GeV [4]. The systematic uncertainty ($\sim$5%) includes the PDF4LHC prescription [5] for the proton parton density function (PDF) and the strong coupling α_S uncertainties using the MSTW2008 68% CL NNLO [6, 7], CT10 NNLO [8, 9] and NNPDF2.3 5f FFN [10]

PDF sets, added in quadrature to the renormalisation and factorisation scale uncertainties. Any deviation of the measured cross section value from the SM prediction could signal the presence of new physics in the top quark production or decay.

2.1.1 Inclusive $t\bar{t}$ cross section measurements

The measurement of the $t\bar{t}$ cross section has been carried out in all the different final states. ATLAS has recently published a measurement of the inclusive $t\bar{t}$ cross section in the dilepton channel using the full data set at $\sqrt{s} = 7$ TeV and $\sqrt{s} = 8$ TeV [11]. The novel feature of this analysis is that the $t\bar{t}$ selection is only based on leptons. By only requiring one electron and one muon with $p_T > 25$ GeV and $|\eta| < 2.5$, a pure sample of $t\bar{t}$ events can be selected. The cross section is measured from the b-jet multiplicity distribution by fitting simultaneously $\sigma_{t\bar{t}}$ and a factor that parametrises the b-jet tagging efficiency and acceptance. For more than one b-jet, the sample is largely dominated by $t\bar{t}$ events as can be seen in the top left plot of Figure 1. The total number of $t\bar{t}$ events is above 33000 with a background fraction of about 10%. The total inclusive $t\bar{t}$ cross section is measured to be:

$$\sigma_{t\bar{t}} = 182.9 \pm 3.1\,(\text{stat.}) \pm 4.2\,(\text{syst.}) \pm 3.6\,(\text{lumi.})\ \text{pb at}\ \sqrt{s} = 7\ \text{TeV}$$

$$\sigma_{t\bar{t}} = 242.4 \pm 1.7\,(\text{stat.}) \pm 5.5\,(\text{syst.}) \pm 3.6\,(\text{lumi.})\ \text{pb at}\ \sqrt{s} = 8\ \text{TeV}$$

The precision of this measurement is 3-4%, as shown in the breakdown of uncertainties summarised in the table of Figure 1. The main systematic uncertainty is due to the knowledge of the luminosity of the data set. For comparisons of this measurement with the theory prediction, an additional uncertainty due to the LHC beam energy (0.6%) needs to be considered which induces an uncertainty on the $t\bar{t}$ cross section of 3-4 pb (1.8%).

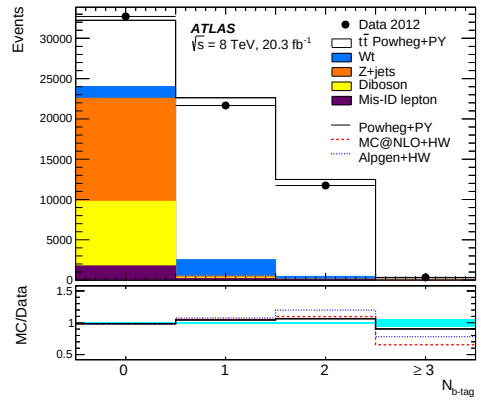

Uncertainties	$\sqrt{s} = 7$ TeV	$\sqrt{s} = 8$ TeV
Statistics	1.7%	0.7%
Analysis systematics	2.3%	2.3%
Luminosity	2.0%	3.1%
Total	3.5%	4.0%

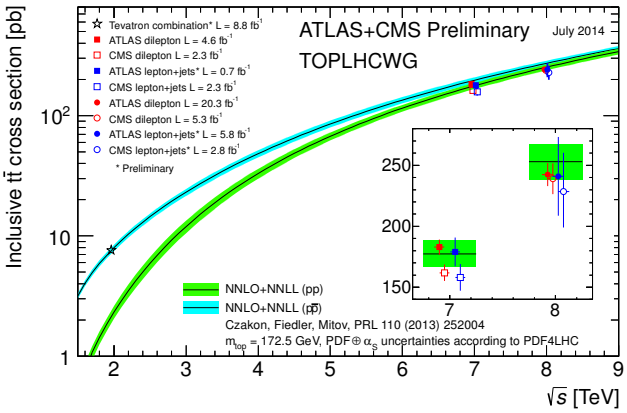

Figure 1: Top left: Multiplicity of b-jets in the selected $t\bar{t}$ dilepton sample at $\sqrt{s} = 8$ TeV. Bottom left: Main uncertainties in the ATLAS $t\bar{t}$ cross section measurements. Right: Summary of $t\bar{t}$ cross section measurements at Tevatron and LHC as a function of the centre-of-mass energy.

The right plot of Figure 1 shows a summary of recent $t\bar{t}$ cross section measurements at Tevatron and LHC compared to NNLO+NNLL QCD. All measurements so far are consistent with the prediction. Overall an impressive experimental precision is accomplished by both Tevatron (6-7%) and LHC (4-6%) measurements, the luminosity uncertainty being the largest at both colliders. The experimental precision matches well the precision reached by the NNLO+NNLL QCD calculation. At $\sqrt{s} = 8$ TeV, the ATLAS and CMS measurements are in good agreement with each other and with the theory prediction, while there is a tension of about two standard deviations at $\sqrt{s} = 7$ TeV.

2.1.2 Differential $t\bar{t}$ cross section measurements

Beyond the inclusive cross section measurements, first measurements of fiducial and differential cross sections have been carried out in the lepton+jets channel at $\sqrt{s}$ =7 TeV. Several observables have been studied: the transverse momentum of the top quark (p_T^t), and the invariant mass (m^{tt}), rapidity (y^{tt}) and transverse momentum (p_T^{tt}) of the $t\bar{t}$ system. The large data sets available at the LHC allow for precise differential measurements reaching high transverse momenta and masses.

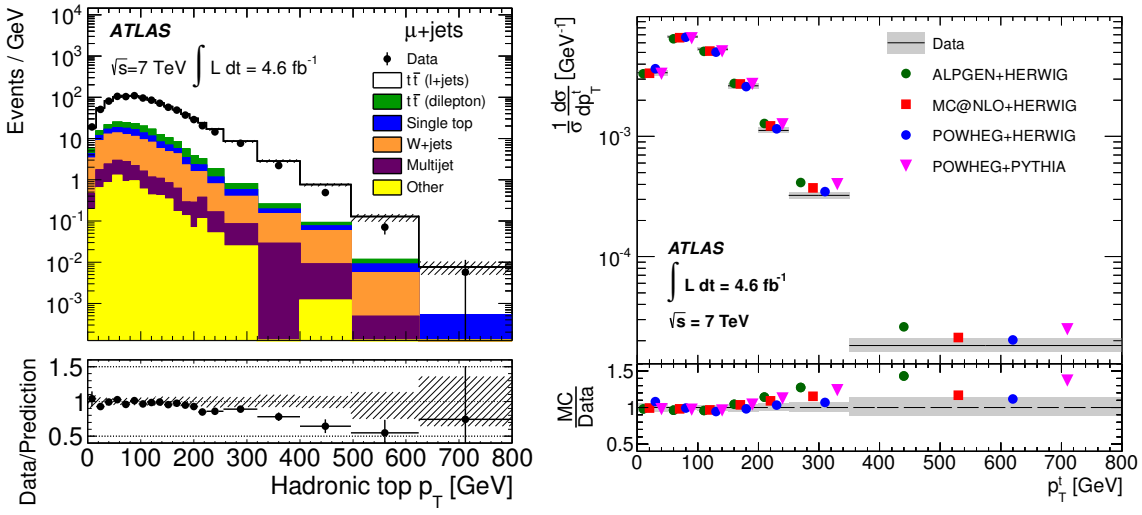

Figure 2: Top pair production cross section as a function of the top quark transverse momentum [12]. In the right plot, data are compared to different fixed order next-to-leading order (NLO) QCD predictions.

The measured kinematic spectra corresponding to individual top quarks as well as to the reconstructed $t\bar{t}$ system show a reasonable (within uncertainties) good agreement with the prediction, with the exception of the high p_T^t tails of the top quark (see left plot of Figure 2) and $t\bar{t}$ system mass where data fall below the prediction [12]. To facilitate the comparison to theoretical predictions, the cross section measurements are defined with respect to the top quarks before the decay (parton level) and after QCD radiation. For that, the measured spectra are corrected for detector efficiency and resolution effects using a regularized unfolding technique. The results are in fair agreement with the predictions of different Monte Carlo (MC) generators in a wide kinematic range. Nevertheless, data distributions are softer than predicted for higher values of the top quark transverse momentum (see right plot of Figure 2) and the mass of the $t\bar{t}$ system. These measurements have also been performed with the CMS detector and a similar behaviour is observed. Possible expla-

nations for these differences are presently being investigated. These include studies with different PDF sets that can soften the gluon distribution, electroweak corrections that can lower the QCD predictions by a few percent, higher order QCD corrections, or effects related to parton shower or hadronisation. In this context it is interesting to point out that PowHeg [13]-[16] interfaced with Herwig [17] for the parton shower is able to describe the data.

2.1.3 Fiducial $t\bar{t}$ cross section measurements

Measurements of final state observables are indispensable to assess and improve the modelling of $t\bar{t}$ events. They need to be defined in a fiducial phase space region close to the detector acceptance and corrected to the level of stable particles, jets and other physics objects entering the detectors. The first fiducial $t\bar{t}$ measurement was published by ATLAS in 2012 [18] and was used to constrain the MC parameters controlling the additional parton radiation in $t\bar{t}$ dilepton events. Events were required to have two b-jets and the additional jets were used to measure the gap fraction which is the probability to emit no jet above a certain p_T cut in a given η region. More radiation will lead to smaller value of this observable. The left distribution of Figure 3 shows this gap fraction observable compared to different MC simulations.

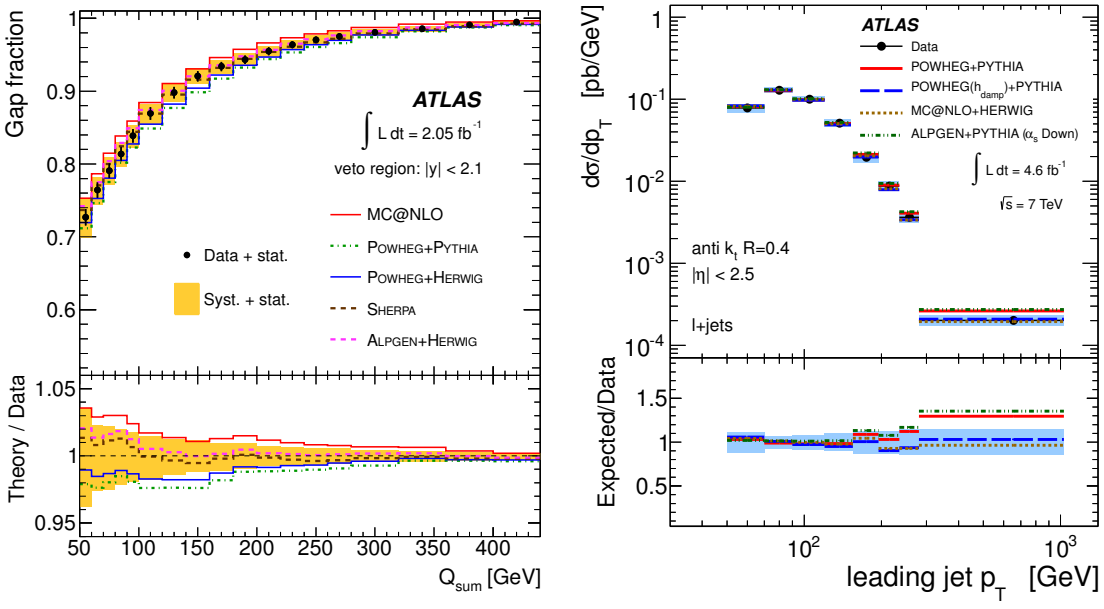

Figure 3: Left: Gap fraction observable as a function of Q_{sum} (scalar sum of the transverse momentum of the additional jets in the rapidity interval) cut applied. Right: The $t\bar{t}$ cross section as a function of the p_T of the leading jet. The data are shown in comparison to different MC predictions. The data points and their corresponding total statistical and systematic uncertainties added in quadrature are shown as a shaded band. The MC predictions are shown with their statistical uncertainty.

In addition, the jet multiplicity and the p_T spectra of the jets have been measured in the lepton+jets channel [19]. Events are required to have at least three jets. The fiducial $t\bar{t}$ production cross section in pp collisions at $\sqrt{s}$ =7 TeV is presented as a function of the jet multiplicity and of the jet p_T separately for each jet up to the fifth jet. The leading jet p_T (right plot of Figure 3) is closely related to the p_T^t, while the fifth jet p_T is related to the p_T of the $t\bar{t}$ system. Thus,

these observables have discriminating power for MC generator models. For the number of jets, the precision is between 10% and 30% with the largest uncertainty at highest jet multiplicity. The measured jet p_T spectra precision varies between 10% and 16%. As already observed for p_T^t, the predictions of PowHeg MC interfaced with Pythia [20] as well as Alpgen [21] are above data at large p_T. However, the leading jet p_T is well described by the MC@NLO [22, 23] MC interfaced with Herwig. This is consistent with the observation that the use of Herwig also leads to a good description of p_T^t as already discussed. However, MC@NLO is softer than data for the fifth jet p_T. Recent investigations show that PowHeg MC with a changed parameter ("hdamp") which controls the additional radiation can describe the data better and also gives a good description of the jet multiplicities.

In conclusion, well defined $t\bar{t}$ final state measurements can be used to understand and reduce the systematic uncertainties associated to the $t\bar{t}$ modelling. This will increase the sensitivity to processes with top quark pairs produced in association with bosons and for many searches of new particles beyond the SM exploiting high jet multiplicities or high p_T regions.

2.2 Single top quarks (electroweak interaction)

Top quarks can also be singly produced via electroweak interactions through the t-channel ($gq \to q't\bar{b}$), associated production with a W boson ($bg \to Wt$) and s-channel ($q\bar{q}' \to t\bar{b}$). After many years of intensive search, the Tevatron experiments reported in 2009 the observation of singly produced top quarks for the first time [24, 25]. At the LHC, the production cross section is significantly higher. The t-channel process dominates and constitutes ∼80% of the total single top quark production cross section, while at Tevatron it was 65%. The predicted production rates for this channel is roughly 30 times more abundant than at the Tevatron. Moreover, background rates rise by a far lower factor with increasing collision energy, leading to an improved signal-to-background ratio. The Wt production is ∼15% at LHC, while it is negligible at the Tevatron. Evidence for the associated Wt production was reported by ATLAS at $\sqrt{s}$ = 7 TeV [26] and the observation has been recently reported by CMS using the full 2012 data set at $\sqrt{s}$ = 8 TeV [27]. For the s-channel production, so far only upper limits are given by the LHC experiments [28], while the Tevatron experiments recently reported the observation of this channel [29].

2.2.1 t-channel cross section

For the t-channel, the signal can be well separated from the background allowing to separate events with top or antitop quarks and to perform the first fiducial and differential measurements. A new measurement of the inclusive t-channel cross section by the ATLAS experiment [30] measured separately the top and antitop cross section at $\sqrt{s}$ = 7 TeV and also the ratio $R_t = \sigma_t/\sigma_{\bar{t}}$:

$$\sigma_t = 46 \pm 1\,(\text{stat.}) \pm 6\,(\text{syst.})\ \text{pb} \quad \text{and} \quad \sigma_{\bar{t}} = 23 \pm 1\,(\text{stat.}) \pm 3\,(\text{syst.})\ \text{pb}$$

$$R_t = 2.04 \pm 0.13\,(\text{stat.}) \pm 0.12\,(\text{syst.})$$

The cross section measurements have a precision of about 12% and the dominant systematic uncertainty is the jet energy uncertainty in the forward detector region (7-8%). This measurement

assumes a top mass m_t = 172.5 GeV and the dependence of the cross section on m_t is also provided. The measurement is in good agreement with NLO QCD [31, 32]. After a basic event selection, the sample is divided in two channels: one with exactly two jets with $p_T > 30$ GeV and $|\eta| < 4.5$ where exactly one jet is b-tagged, and another with three jets being one or two b-tagged. For each channel, kinematic variables of the reconstructed physics objects are combined in a neural network to discriminate signal from background (see left plot of Figure 4). Applying a cut on the neural network output, a high purity region is defined to measure the differential cross sections as a function of the top and antitop transverse momentum and rapidity. The right distribution of Figure 4 shows the single top t-channel cross section as a function of p_T^t. NLO QCD calculation gives a good description of the measurement.

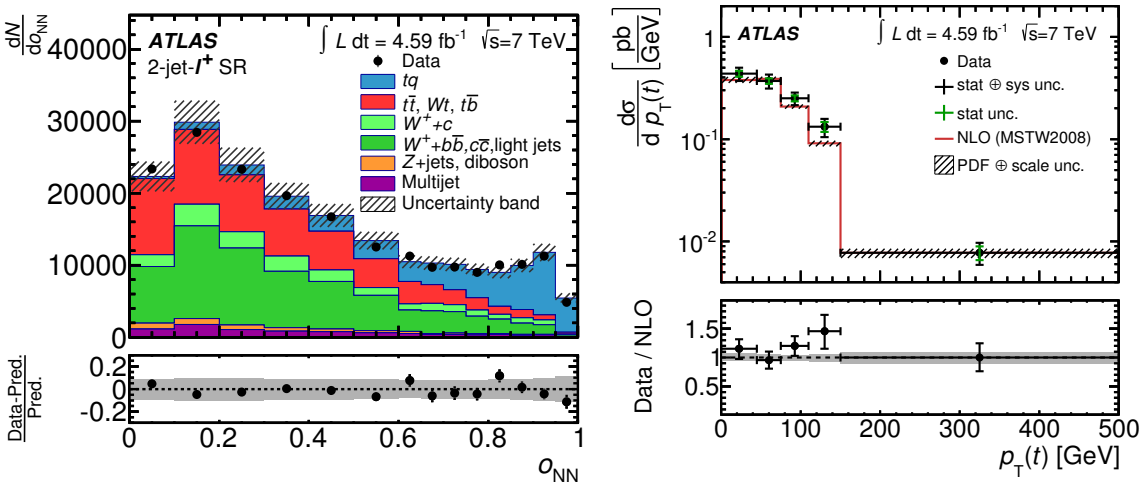

Figure 4: Left: Neural network output for the t-channel single top quark cross section measurement. Right: Single top production cross section in the t-channel as a function of the top quark transverse momentum compared to a NLO QCD prediction [30].

A first preliminary fiducial cross section measurement for single top production defined using stable particles within the detector acceptance has been presented by ATLAS for $\sqrt{s}$ = 8 TeV [33]. The benefit of measuring a production cross section within a fiducial volume is that uncertainties connected with event generation can be reduced to differences within the fiducial volume. Differences between generators, hadronisation models or PDFs can be separated into components visible in the measured phase space and in the non-visible phase space. The fiducial phase space is defined by the reconstructed physics objects in the detector. The fraction of t-channel signal events in this phase space is obtained from a likelihood fit to a neural network discriminant based on kinematic variables. The precision of the fiducial cross section measurement is 14%, being the choice of the t-channel generator (8%) and the jet energy measurement in the forward region of the detector (8%) the largest uncertainties. Using various MC generator models, the fiducial cross section can be extrapolated to the full phase space and can be compared to the NLO+NNLL calculation. There is an additional uncertainty on the extrapolation due to the choice of the PDF set (3.8%). A summary of these inclusive cross sections is presented on the left side of Figure 5. The values deduced with the acceptances obtained with the NLO generators PowHeg and aMC@NLO [34] are in excellent

agreement with the NLO+NNLL prediction and have only a difference of 1.7% to each other.

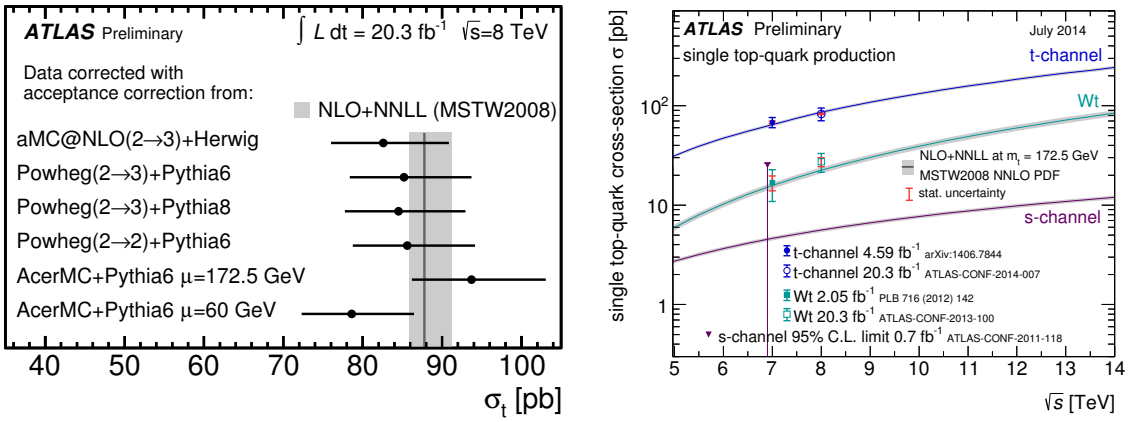

Figure 5: Left: Inclusive t-channel single top quark production cross section obtained from extrapolating the fiducial cross section to the full phase space using the acceptance of different MC generators. The vertical line indicates the NLO+NNLL theoretical cross section, including the uncertainty displayed as a grey band. Right: Summary of the single top quark production cross section measurements in ATLAS. For the s-channel only an upper limit is given.

The right plot of Figure 5 summarises the present status of the electroweak production of top quarks in ATLAS. With the observation of the s-channel process at Tevatron, all single top processes are now established. The focus now is on measuring the production cross section precisely with the least possible model dependence. A first step in this direction has been made by measuring fiducial cross section to factorize experimental uncertainty from theory uncertainty connected to the extrapolation of the detector acceptance to the full phase space.

3. Top quark properties

3.1 Top mass measurements

The standard way to measure the top mass is to reconstruct the top quark decay products (W boson and b quark) and to form the invariant mass. The measurement is calibrated using MC simulations and therefore the result refers to the mass as implemented in the simulations. The selection of top quarks is done by identifying the final state objects from the decay of the top quark using simple combinations of the physics objects in the event or more sophisticated techniques using kinematic fits based on likelihoods or χ^2 metric, and exploiting the known value of the W boson mass to constrain physics and detector effects. There are different techniques such as the template, the ideogram and the matrix element methods. In ATLAS, the template method is commonly used. The simplest version only fits m_t and the reconstructed top mass is obtained fitting the distribution of m_t in data to reference MC templates for various top masses. However, the most precise measurement in ATLAS is obtained with a three-dimensional fit [35]. In addition to m_t, a global jet energy scale factor (JSF) and a relative b-jet to light-jet energy scale factor (bJSF) are constraint. The top quark mass is measured to be $m_t = 172.31 \pm 0.23$ (stat.) $\pm$ 0.72 (JSF + bJSF) $\pm$ 1.35 (syst.) GeV, where the uncertainties labelled JSF and bJSF refer to the statistical uncertainties on m_t induced by

the in-situ determination of these scale factors.

Over the past years, several top mass measurements have been carried out by the Tevatron and LHC experiments. Improving the detector performance, the signal MC modelling and the measurement techniques, the m_t measurements became increasingly precise. In March 2014, the first world combination of m_t was carried out by the ATLAS, CMS, D0 and CDF collaborations [36] and the world average obtained is $m_t = 173.34 \pm 0.27$ (stat.) $\pm$ 0.24 (JSF + bJSF) $\pm$ 0.67 (syst.) GeV, with a relative precision of 0.44%. Figure 6 shows a summary of the m_t measurements entering in the world combination. Since the world average m_t combination, several new measurements with higher precision were published. The highest precision is reached for the lepton+jets channel (0.43%), but also the dilepton channel (0.67%) and the fully hadronic channel (0.80%) give a good precision.

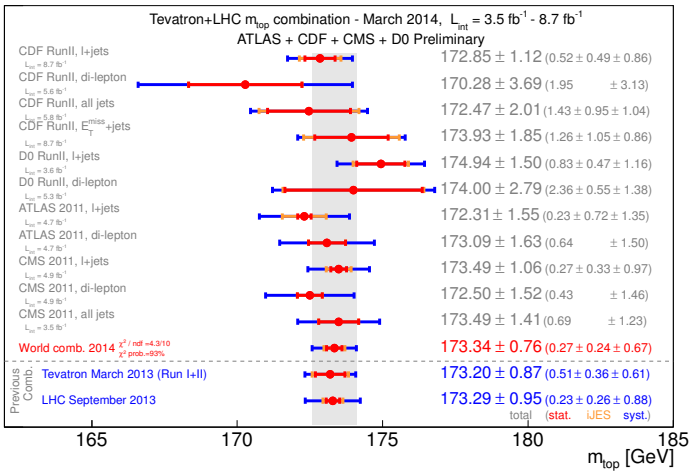

Figure 6: Comparison of the world m_t combination result with the individual m_t determinations per $t\bar{t}$ decay channel, experiment and collider. The grey band reflects the total uncertainty on the combined m_t value.

Top mass measurements methods reconstructing the top decay products might suffer from uncertainties of the order of Λ_{QCD}. There are also ongoing discussions on how to interpret the MC-based results in terms of the m_t parameter in the SM Lagrangian. It is thus also important to measure m_t using alternative techniques like the comparison of NNLO+NNLL QCD calculations to the inclusive $t\bar{t}$ production cross section measurements [11] or to observables based on $t\bar{t}$+jets events [37, 38]. Since this QCD calculation uses the pole mass scheme, the m_t^{pole} can be determined. In this case, the precision obtained is of 1.5% being the largest experimental uncertainty due to the luminosity of the data set.

3.2 Spin correlations

Although the top and antitop quarks produced via the strong interaction at the hadron colliders are unpolarized, their spins are correlated. New physics models beyond the SM can change the spin correlation of the top and the antitop quark by either changing the spin of the their decay products, or by changing the production mechanism of the $t\bar{t}$ pair. The strength of the correlation can be

expressed as the asymmetry $A = \frac{N_{\Uparrow\Uparrow}+N_{\Downarrow\Downarrow}-N_{\Uparrow\Downarrow}-N_{\Downarrow\Uparrow}}{N_{\Uparrow\Uparrow}+N_{\Downarrow\Downarrow}+N_{\Uparrow\Downarrow}+N_{\Downarrow\Uparrow}}$ between the number of events with parallel spins, $N_{\Uparrow\Uparrow}$ and $N_{\Downarrow\Downarrow}$, and the number of events with antiparallel spins, $N_{\Uparrow\Downarrow}$ and $N_{\Downarrow\Uparrow}$, which depend on the choice of the quantization axis, referred to as "spin basis".

The extremely short lifetime of the top quark allows to study the spin at its production through the angular distributions of its decay products. The differential distribution of the decay width, $d\Gamma/d|\cos\theta_{\pm}|$, is proportional to the cosine of the angle $\theta_{\pm}$ between the positively (negatively) down-type fermion from the W boson, which in the case of a leptonic decay allows for very clean measurements, from the top (antitop) quark decay and the top (antitop) quark spin quantization axis in the top (antitop) quark rest frame. The spin correlation is expressed by the double differential cross section:

$$\frac{1}{\sigma}\frac{d^2\sigma}{d[cos\ \theta_+\ cos\ \theta_-]} = \frac{1}{4}(1 + \alpha_+ P_+ cos\ \theta_+ + \alpha_- P_- cos\ \theta_- + A\alpha_+\alpha_- cos\ \theta_+ cos\ \theta_-) \quad (3.1)$$

where α represents the spin analysing power and $P_{\pm}$ is the polarisation of the top (antitop) quark. Since $\alpha \approx 1$ at leading order (LO) for charged leptons, these final state particles are commonly used for these measurements. As spin quantization axis, the helicity basis[1] of the top quark is used since it is well defined and there are theoretical predictions.

The full 2011 data set recorded by the ATLAS detector at $\sqrt{s}$ = 7 TeV has been analysed to check the compatibility with the SM spin correlation strength prediction [39]. Four different observables are investigated, which are different linear combinations of components in the spin density matrix of $t\bar{t}$ production: the azimuthal difference $\Delta\phi$ of the charged lepton momentum directions in the laboratory frame, the ratio of the squares of matrix elements for top quark pair production and decay from the fusion of like-helicity gluons with and without spin correlation at LO (S-ratio), and the product of $\cos\theta_+ \cos\theta_-$ in both the helicity basis and the so called maximal basis[2], which maximizes the value of the spin correlation strength. A template fit is performed for all four observables to extract the spin correlation strength. The fit includes a linear superposition of the distribution from the SM $t\bar{t}$ MC simulation with coefficient $f_{\rm SM}$, and from the uncorrelated $t\bar{t}$ MC with coefficient (1 - $f_{\rm SM}$). The left plot of Figure 7 shows the measured $f_{\rm SM}$ for the four different observables. To get the measured spin correlation strength, the $f_{\rm SM}$ obtained from the fit has to be multiplied by the SM prediction. The dominant systematic uncertainties affecting these measurements come from $t\bar{t}$ modelling.

3.3 Charge asymmetry

The $t\bar{t}$ production is predicted to be symmetric under charge conjugation at LO in the SM. At NLO, however, for the $q\bar{q}$ and qg production modes, there is a small preference to produce top (antitop) quarks in the direction of the incoming quark (antiquark) in the partonic rest frame. At the Tevatron, this asymmetry is equivalent to a forward-backward asymmetry, with top (antitop) quarks more abundant in the direction of the incoming proton (antiproton). At the LHC, this

[1] The SM prediction for the helicity basis is $A_{\rm hel}$ = 0.31 at 7 TeV.

[2] No prediction from the SM exists for the asymmetry A in the maximal basis, so the prediction from the MC@NLO MC generator $A_{\rm max}$ = 0.44 was used.

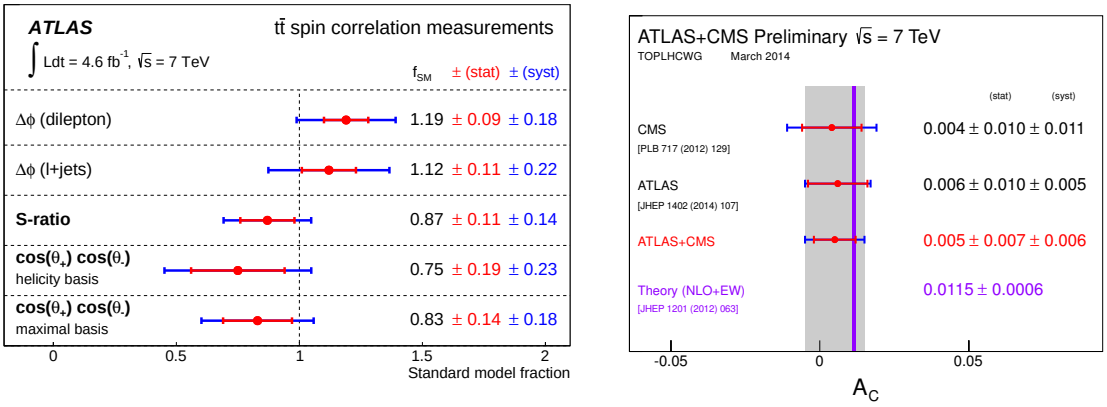

Figure 7: Left: Summary of the measurements of the fraction of $t\bar{t}$ events corresponding to the SM spin correlation hypothesis, f_{SM}, using four spin correlation observables sensitive to different properties of the production mechanism. The dashed vertical line at $f_{\mathrm{SM}} = 1$ indicates the SM prediction. The inner red error bars indicate statistical uncertainties, the outer blue error bars indicate the contribution of the systematic uncertainties to the total uncertainties. Right: Summary of the single measurements and the LHC combination of the $t\bar{t}$ charge asymmetry compared to the theory prediction (calculated at NLO including electroweak corrections). The grey band illustrates the total uncertainty of the combined result.

forward-backward asymmetry vanishes trivially because the pp initial state (dominated by gluon-gluon fusion) is symmetric. Nevertheless, QCD predicts a slight preference for centrally produced antitop quarks at the LHC, while top quarks are more abundant at large positive and negative rapidities. This is due to the proton composition in terms of quarks and antiquarks: quarks carry a large momentum fraction while antiquarks carry a small momentum fraction. Thus, the boost into the laboratory frame "squeezes" top quarks mainly in the forward and backward directions, while antitop quarks are left in the central region. It is therefore useful to define the following charge asymmetry $A_C = \frac{\Delta|y|>0 - \Delta|y|<0}{\Delta|y|>0 + \Delta|y|<0}$ with $\Delta|y| = |y_t| - |y_{\bar{t}}|$, making use of the difference of absolute rapidities $|y_t|$ and $|y_{\bar{t}}|$ of top and antitop quarks. At NLO in the SM, this asymmetry is expected to be 0.0115 ± 0.0006 for pp collisions at $\sqrt{s} = 7$ TeV [40]. ATLAS measured this charge asymmetry in $t\bar{t}$ lepton+jets events using the full 2011 data set [41]. The reconstructed $\Delta|y|$ distribution was unfolded to parton level and the measured value for the asymmetry is found to be of $0.006 \pm 0.010(\mathrm{stat.}) \pm 0.005(\mathrm{syst.})$. Furthermore, a combination with the results of the CMS experiment has been performed and is presented in the right plot of Figure 7 [42].

3.4 Couplings

The top quark couples to other SM fields through its gauge and Yukawa interactions. The coupling of the top quark to the W boson can be examined either by looking at the decay of the top quark or from single top quark production. With the advent of large data samples with top quarks at the LHC, the processes where bosons (γ, Z or H) are produced in association with top quarks become accessible. The first evidence on the couplings of the top quark to these particles (will) come from the production rate of these processes. In this direction, several dedicated and sophisticated analyses are being performed in ATLAS.

3.4.1 Top + W

In the SM the top quark decays through an electroweak interaction almost exclusively to a W boson and a b quark. The magnitude of the Wtb coupling is proportional to the Cabibbo-Kobayashi-Maskawa (CKM) matrix element V_{tb} and is therefore almost equal to one, reflecting the vector ($\bar{\psi}\gamma^{\mu}\psi$) minus axial ($\bar{\psi}\gamma^{\mu}\gamma^{5}\psi$) structure of the Wtb vertex. One way of probing the structure of this vertex is to study the W bosons produced in the decay of top quarks which can have longitudinal, left-handed or right-handed polarizations with fractions F_0, F_L and F_R respectively. At NNLO in the SM, they are predicted to be 0.687±0.005, 0.311±0.005 and 0.0017±0.0001 [43] and they have been measured in the Tevatron and LHC experiments. The W boson helicity fractions can be extracted from a direct fit to the angular distribution of top quark decay products, $\cos\theta$, using templates from MC simulations. Alternatively, angular asymmetries (A_+, A_- and A_{FB}), built from $\cos\theta$, were also used by ATLAS [44]. The angle θ is defined between the momentum of the charged lepton in the W boson rest frame and the W boson momentum in the top quark rest frame. ATLAS measured the helicity fractions to be F_0 = 0.67±0.03(stat.)±0.06(syst.), F_L = 0.32±0.02(stat.)±0.03(syst.) and F_R = 0.01±0.01(stat.)±0.04(syst.). All these measurements are consistent with the SM expectations and were used to probe the existence of anomalous Wtb couplings. Exclusion limits on the real components of the anomalous couplings g_L and g_R (left- and right-handed tensor couplings) were set at 68% and 95% confidence level, as shown in the left plot of Figure 8. The region of g_R around 0.8 is disfavoured by the current experimental measurements on the single top quark production cross sections at the Tevatron and the LHC.

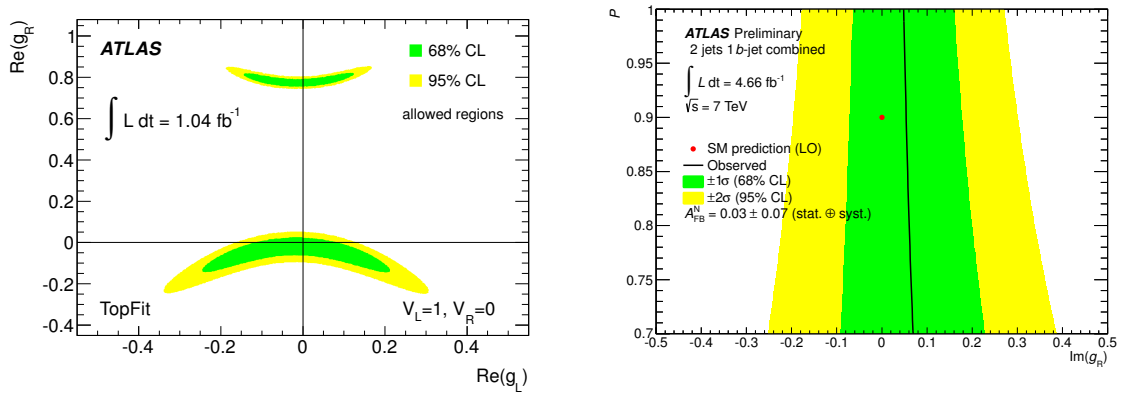

Figure 8: ATLAS allowed 68% and 95% confidence level regions on the real part of the anomalous couplings g_L and g_R derived from the W boson helicity fractions measured in $t\bar{t}$ events (left) and on the top quark polarisation-Im(g_R) plane obtained from the A_{FB}^N measurement in single top quark events (right).

In the presence of polarised top quarks, such as those produced via the electroweak interaction, one can also exploit the spin direction and define further references normal and transverse to the plane formed by the W boson momentum and the top quark spin direction. In a similar way that the angle θ is defined between the lepton in the W boson rest frame and the momentum of the W boson, the angles θ_N and θ_T can be defined between the lepton from the W boson and these new directions. The most interesting remark is that the normal set of polarisation fractions (F_0^N, F_L^N and F_R^N) depend on the imaginary part of the anomalous coupling g_R, so observables depending on these deserve

special attention. If CP symmetry is conserved in the Wtb vertex, i.e. if all anomalous couplings are real, then $F_L^N = F_R^N$, and a net normal W polarisation ($F_L^N \neq F_R^N$) can only be produced if CP is violated in the top quark decay. This property is unique of the normal direction and it has been explored in ATLAS using t-channel single top quark events collected in 2011 [45]. The observable chosen was the forward-backward asymmetry A_{FB}^N built from the angular distribution $\cos\theta_N$ and has allowed to set the first experimental limit on the imaginary part of g_R as shown in the right plot of Figure 8. This measurement is limited by the statistical uncertainty and systematic uncertainties related to the modelling of the t-channel signal process.

3.4.2 Top +γ

At hadron colliders, a measurement of the $t\bar{t}\gamma$ coupling via $q\bar{q} \to \gamma \to t\bar{t}$ is unrealistic due to the overwhelming contribution from QCD processes. Therefore, a more feasible approach to probe the $t\bar{t}\gamma$ coupling (and therefore the top quark electric charge) is via the measurement of associated production of a photon with a top quark pair. At the time of writing, the ATLAS collaboration reported the observation of this process [46]. The $t\bar{t}\gamma$ production cross section times the branching ratio of the lepton+jets $t\bar{t}$ decay channel is measured in a fiducial kinematic region within the ATLAS acceptance: $\sigma_{t\bar{t}\gamma}^{fid} = 63 \pm 8$ (stat.) $^{+17}_{-13}$ (syst.) $\pm$ (lumi.) fb per lepton flavour, in agreement with the NLO prediction. The main background contribution originates from hadron fakes, and the dominant systematic uncertainty is due to the photon identification efficiency.

3.4.3 Top + V (Z or W)

The primary source of information on the $t\bar{t}Z$ coupling at hadron colliders is the observation of the associated production of a Z boson and top quark pair. This process can include the Z boson as initial state radiation (ISR), i.e. radiated from the incoming quarks, or as final state radiation (FSR), i.e. radiated from the top or antitop quarks. Only the latter processes are sensitive to the weak neutral current top coupling (and the weak isospin of the top quark). In contrast to $t\bar{t}Z$, the associated W boson in $t\bar{t}W$ does not couple to the top quark, but is radiated from the incoming quarks (ISR process). The ISR processes are similar for $t\bar{t}Z$ and $t\bar{t}W$, thus the understanding of the $t\bar{t}W$ production could be useful to disentangle the ISR from the FSR contribution in the $t\bar{t}Z$ processes.

Depending on the decay of the bosons and the number of leptons and jets in the final state, several experimental signatures can be explored. The early ATLAS results at $\sqrt{s}$ = 7 TeV used the three leptons channel and only reported an upper limit on the cross section $\sigma_{t\bar{t}Z} < 0.71$ pb at 95% confidence level [47]. Evidence for both $t\bar{t}Z$ and $t\bar{t}W$ production at $\sqrt{s}$ = 8 TeV has been recently announced by both the ATLAS and CMS collaborations by combining different final state channels and measuring $\sigma_{t\bar{t}Z}$, $\sigma_{t\bar{t}W}$ and $\sigma_{t\bar{t}V}$ from a profile likelihood fit [48]. The ATLAS search includes final states with three and two leptons and measures these cross sections relative to the NLO prediction: $\mu_{t\bar{t}Z} = \sigma_{t\bar{t}Z}/\sigma_{t\bar{t}Z}^{SM} = 1.25^{+0.57}_{-0.48}$ for $t\bar{t}Z$, $\mu_{t\bar{t}W} = \sigma_{t\bar{t}W}/\sigma_{t\bar{t}W}^{SM} = 0.73^{+0.29}_{-0.26}$ for $t\bar{t}W$ and $\mu_{t\bar{t}V} = \sigma_{t\bar{t}V}/\sigma_{t\bar{t}V}^{SM} = 0.89^{+0.23}_{-0.22}$ for $t\bar{t}V$ (see left plot of Figure 9). These measurements correspond to an observed 3.2, 3.1 and 4.9 standard deviations excess over the background-only hypothesis respectively.

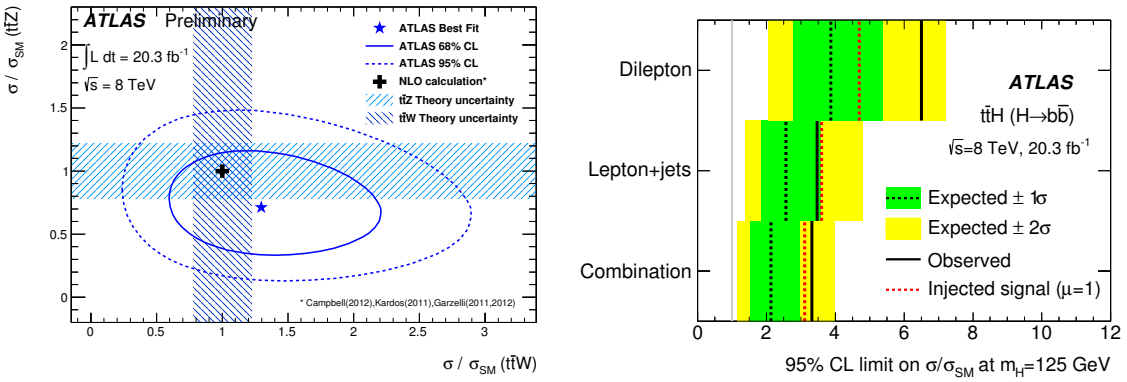

Figure 9: Left: Result of the combined simultaneous measurement of $t\bar{t}Z$ and $t\bar{t}W$ signal strengths. The dashed area corresponds to the 22% uncertainty on the NLO QCD predictions. Right: Observed and expected 95% confidence level upper limits on the $t\bar{t}H$ production cross section for the individual final states and the combination. The lines denoted "SM signal injected" show the expected 95% confidence level upper limit for a data set corresponding to the background-plus-SM $t\bar{t}H$ production.

3.4.4 Top + *H*

Indirect evidence of the top quark Yukawa coupling comes from the Higgs boson production via gluon-gluon fusion which is predicted to proceed predominantly through a loop with top quarks. The decay of the Higgs to photons provides complementary information. The observation of $t\bar{t}H$ production will allow for direct access to this coupling. Searches are being performed for the production of the Higgs boson in association with pairs of top quarks exploiting multiple Higgs decay modes, including decays into pairs of b quarks, vector bosons, taus and photons. No significant excess is found and the limit and μ values are compatible with the SM prediction, as can be seen in the right plot of Figure 9 [49, 50, 51].

4. Conclusions

The LHC Run 1 data have allowed to perform very precise measurements involving top quarks and triggered tremendous activities on both the experimental and theoretical side. The experimental precision achieved in the top quark pair cross section measurements (3-4%) is at the same level of the precision of the latest NNLO+NNLL QCD calculations. First differential and fiducial cross section measurements have become available for $t\bar{t}$ and single top quark production. The differential measurement of the top quark transverse momentum and the mass of the top pair system in $t\bar{t}$ events show that the data fall significantly below the QCD predictions. At present, this effect is being investigated. The t-channel process of the electroweak production is measured with a precision of about 12%. Processes where top quarks are produced in association with bosons (γ, Z or H) are becoming accessible. The first observation of $t\bar{t}\gamma$ process and first evidence of $t\bar{t}Z$ and $t\bar{t}W$ have been recently reported. Many more detailed studies of top quark properties have been published. Most measurements are already dominated by systematic uncertainties. No deviations from the SM predictions have been observed so far.

References

[1] The ATLAS Collaboration, *JINST* **3** S08003 (2008).
[2] The CMS Collaboration, *JINST* **3** S08004 (2008).
[3] J. Beringer *et al.* (Particle Data Group), *Phys. Rev. D* **86** 010001 (2012).
[4] M. Czakon, P. Fiedler, A. Mitov, *Phys. Rev. Lett.* **110** 252004 (2013).
[5] M. Botje *et al.*, arXiv: 1101.0538 (2011).
[6] A. D. Martin *et al.*, *Eur. Phys. J.* **C63**, 189 (2009).
[7] A. D. Martin *et al.*, *Eur. Phys. J.* **C64**, 653 (2009).
[8] H.-L. Lai *et al.*, *Phys. Rev. D* **82** 074024 (2010).
[9] J. Gao *et al.*, *Phys. Rev. D* **89** 033009 (2014).
[10] R. D. Ball *et al.*, *Nucl. Phys.* **B867** 244 (2013).
[11] The ATLAS Collaboration, *Eur. Phys. J.* **C74** 3109 (2014).
[12] The ATLAS Collaboration, *Phys. Rev. D* **90**, 072004 (2014).
[13] S. Frixione *et al.*, *JHEP* **0709**, 126 (2007).
[14] P. Naxon *et al.*, *JHEP* **0411**, 040 (2004).
[15] S. Frixione *et al.*, *JHEP* **0711**, 070 (2007).
[16] S. Alioli *et al.*, *JHEP* **1006**, 043 (2010).
[17] G. Corcella *et al.*, *JHEP* **0101**, 010 (2001).
[18] The ATLAS Collaboration, *Eur. Phys. J.* **C72**, 2043 (2012).
[19] The ATLAS Collaboration, *JHEP* **01**, 020 (2015).
[20] T. Sjostrand *et al.*, *JHEP* **05**, 026 (2006).
[21] M. L. Mangano *et al.*, *JHEP* **0307**, 001 (2003).
[22] S. Frixione *et al.*, *JHEP* **0206**, 029 (2002).
[23] S. Frixione *et al.*, *JHEP* **0308**, 007 (2003).
[24] The CDF Collaboration, *Phys. Rev. Lett.* **103** 092002 (2009).
[25] The D0 Collaboration, *Phys. Rev. Lett.* **103** 092001 (2009).
[26] The ATLAS Collaboration, *Phys. Lett.* **B** 716 (2012) 142-159.
[27] The CMS Collaboration, *Phys. Rev. Lett.* **112** 231802 (2014).
[28] The ATLAS Collaboration, ATLAS-CONF-2011-118, http://cds.cern.ch/record/1376410 (2011).
[29] The CDF and D0 Collaborations, *Phys. Rev. Lett.* **112** 231803 (2014).
[30] The ATLAS Collaboration, *Phys. Rev. D* **90** 112006 (2014).
[31] P. Kant *et al.*, arXiv: 1406.4403 (2014).
[32] J. M. Campbell *et al.*, *Phys.Rev.Lett.* **102** 182003 (2009).
[33] The ATLAS Collaboration, ATLAS-CONF-2014-007, https://cds.cern.ch/record/1668960 (2014).
[34] J. Alwall *et al.*, *JHEP* **1407**, 079 (2014).
[35] The ATLAS Collaboration, ATLAS-CONF-2013-046, https://cds.cern.ch/record/1547327 (2013).
[36] The ATLAS, CDF, CMS and D0 Collaborations, arXiv: 1403.4427 (2014).
[37] S. Alioli *et al.*, *Eur. Phys. J.* **C73** 2438 (2013).
[38] The ATLAS Collaboration, ATLAS-CONF-2014-053, https://cds.cern.ch/record/1951319 (2014).
[39] The ATLAS Collaboration, *Phys. Rev. D* **90** 112016 (2014).
[40] W. Bernreuther *et al.*, *Phys. Rev. D* **86** 034026 (2012).
[41] The ATLAS Collaboration, *JHEP* **02** 107 (2014).
[42] The ATLAS and CMS Collaborations, ATLAS-CONF-2014-012, https://cds.cern.ch/record/1670535 (2014).
[43] A. Czarnecki *et al.*, *Phys. Rev. D* **81** 111503 (2010).
[44] The ATLAS Collaboration, *JHEP* **1206** 088 (2012).
[45] The ATLAS Collaboration, ATLAS-CONF-2013-032, https://cds.cern.ch/record/1527128 (2013).
[46] The ATLAS Collaboration, arXiv: 1502.00586, submitted to *Phys. Rev. D* (2015).
[47] The ATLAS Collaboration, ATLAS-CONF-2012-126, https://cds.cern.ch/record/1474643 (2012).
[48] The ATLAS Collaboration, ATLAS-CONF-2014-038, https://cds.cern.ch/record/1735215 (2014).
[49] The ATLAS Collaboration, *Phys. Lett.* **B** 740 (2015) 222-242.
[50] The ATLAS Collaboration, arXiv: 1503.05066, submitted to *Eur. Phys. J.* **C** (2015).
[51] The ATLAS Collaboration, ATLAS-CONF-2015-006, https://cds.cern.ch/record/2002125 (2015).